Submitted to: GCH

Pyrolusite Surface Transformations Measured in Real-Time During the Reactive Transport of Co(II)EDTA

Scott Fendorf[1]*, Philip M. Jardine[2], Ronald R. Patterson[1], David L. Taylor[2], and Scott C. Brooks[2]

[1]Soil Science Division, University of Idaho, Moscow, ID 83844-2339

[2]Environmental Science Division, Oak Ridge National Laboratoj, Oak Ridge, TN 37831

*Corresponding Author:
Phone: (208) 885-676
FAX: (208) 885-7760
Email: fendorf@uidaho.edu

Pyrolusite Surface Transformations Measured in Real-Time During the Reactive Transport of Co(II)EDTA

Abstract--Oxidation of $Co(II)EDTA^{2-}$ to $Co(III)EDTA^{-}$ by manganese and iron hydrous oxide minerals enhances the transport of ^{60}Co in subsurface environments. Reduction of the proposed oxidant MnO_2 has not been identified in hydrodynamic systems, leaving the fate and transport mechanisms involving ^{60}Co in natural environments unresolved. We investigated the transport of $Co(II)EDTA^{2-}$ through packed beds of β-MnO_2 and identified the reaction mechanism using a novel hydrodynamic flow cell coupled with XANES spectroscopy. Using this technique we are able to determine both solution and solid-phase species of cobalt and manganese in real-time. The source of $Co(II)EDTA^{2-}$ oxidation is Mn(IV), which is reduced to Mn(III). Once produced, Mn(III) forms an α-Mn_2O_3-layer on pyrolusite that passivates the surface after an initial reaction period and ultimately limits the production of $Co(III)EDTA^{-}$. As a consequence, the enhanced transport of ^{60}Co by oxidative processes may be diminished upon continual exposure to pyrolusite-an advantageous finding from an environmental quality perspective. Furthermore, Mn(III) is formed rather than Mn(II), with a resulting stable trivalent manganese solid (α-Mn_2O_3).

1. INTRODUCTION

The migration of radionuclides away from low-level waste disposal facilities poses a threat to human and animal health (Francis et al., 1980; Killey et al., 1984; Olsen et al., 1986). Unfortunately, movement of these hazardous compounds has been documented over a broad geographical range from Oak Ridge, TN (Olsen *et al.*, 1986) to West Valley, NY (Francis *et al.*, 1980), to the Canadian burial grounds at the Chalk River Nuclear Labs (Killey *et al.*, 1984). Enhanced migration of the radionuclide ^{60}Co in subsurface environments is attributed to the presence of synthetic organic chelating agents, such as ethylenediaminetetraacetic acid (EDTA) (Killey et al., 1984; Olsen et al., 1986; Means et al., 1978). Compounding the problem of ^{60}Co mobility is the possible oxidation of $Co(II)EDTA^{2-}$ to $Co(III)EDTA^{-}$ by soil and subsurface materials (Szecsody et al., 1994; Jar-dine and Taylor, 1995; Zachara et al., 1995b; Brooks et al., 1996). The stability of Co-EDTA complexes changes dramatically depending upon the valence state of Co; the stability constant for $Co(III)EDTA^{-}$ (log $K_{Co(III)EDTA}$ = 39.8) increases by a factor greater than 10^{20} relative to $Co(II)EDTA^{2-}$ (log $K_{Co(II)EDTA}$ = 18.2). The environmental significance of $^{60}Co(III)EDTA^{-}$ is pronounced since this species is extremely stable and devoid of abiotic and microbial degradation pathways.

Hydrous manganese oxides (Jardine et al., 1995; Zachara et al., 1995a) and to a lesser extent iron oxides (Brooks et al., 1996; Xue and Traina., 1996) are presumed to be the dominant oxidants of $Co(II)EDTA^{2-}$ in natural environments. Manganese oxides in particular have the ability to rapid oxidize $Co(II)EDTA^{2-}$ to $Co(III)EDTA^{-}$. Jardine and Taylor (1995) have demonstrated that $Co(II)EDTA^{2-}$ is rapidly oxidized to Co(III)EDTA during transport through pyrolusite (ß-MnO_2)-coated quartz sand columns, and Zachara et al. (1995a) linked the oxidative transformation of $Co(II)EDTA^{2-}$ to Mn-oxides present in natural sediments. However, reduction of the proposed oxidant, MnO_2, has not been

identified in hydrodynamic systems, leaving the fate and transport mechanisms involving ^{60}Co in natural environments unresolved (Jardine and Taylor, 1995).

Divalent Mn is often assumed to result from the reduction of W-dioxides (Murray et al., 1968; Murray and Dillard, 1979); it has also been speculated that a Mn(III) solid phase is formed during reduction of Mn(IV)-oxides. Jardine and Taylor (1995) reported the reversible loss of the oxidative potential of MnO_2 with continual exposure to $Co(II)EDTA^{2-}$, and they demonstrated that the accumulation of Mn^{2+} on the oxide surface did not explain the loss in oxidative potential. Rather, they hypothesized that the formation of a thin layer of Mn_2O_3 on the MnO_2 surface resulted in the loss of oxidative capacity. To potentially identify the Mn reaction products, we recently analyzed solids extruded from pyrolusite columns after reaction with $Co(II)EDTA^{2-}$ for varying lengths of time using X-ray absorption near-edge (XANES) spectroscopy (Fendorf et al., 1998). On the basis of reconstructing the reacted pyrolusite XANES spectrum with a combination of Mn mineral spectra (including all known forms of Mn(III) hydrous oxides), we confirmed the formation of a Mn(III) solid on pyrolusite-present as an α-Mn_2O_3-like phase. This finding is consistent with x-ray photoelectron spectroscopy which indicated the production of Mn(III) after bimessite is reacted with Co(II) (Crowther et al., 1983). The production of Mn(III) is also noted in the oxidation of Mn(II) as either a transient intermediate phase, dominantly Mn_3O_4 or β-MnOOH, or as a stable end product, γ-MnOOH (Hem, 1981; Hem et al., 1982; Hem and Lind, 1983; Murray et al., 1985).

What remains to be known about the reaction between $Co(II)EDTA^{2-}$ and pyrolusite is the time-dependent formation of the Mn(III) phase; particularly helpful

would be the direct (in *situ*) identification of both Co and Mn transformations simultaneously. Information provided by such measurements would enable the reaction mechanism between $Co(II)EDTA^{2-}$, resolving whether in fact the α-Mn_2O_3 phase forms coincident with the loss in pyrolusite's oxidative capacity toward $Co(II)EDTA^{2-}$. Without knowledge of the reduced products, there is an incomplete mechanistic understanding of the governing reactions, thus limiting the generic applicability of the observations.

In response to this need, we developed a novel experimental approach combining a hydrodynamic reaction cell with XANES spectroscopy to measure changes in Mn species upon exposure of β-MnO_2 to $Co(II)EDTA^{2-}$. Additionally, solution species are measured concurrently with the solid-phase. The oxidation of $Co(II)EDTA^{2-}$ to $Co(III)EDTA^{-}$ by Mn (oxide) minerals is believed to be a surface-mediated phenomena that affects only the outer molecular layer(s) of the mineral. Accordingly, our experiments used thin films (only a few monolayers thick) of pyrolusite on an inert silica substrate to provide surface sensitivity. In combination, our experimental approach thus measures aqueous and solid species of Co and Mn, with surface sensitivity, in real-time under hydrodynamic conditions.

2. EXPERIMENTAL METHODS

2.1 Synthesis of Silica Coated Pyrolusite

XANES spectroscopy is inherently a bulk technique that is not surface sensitive without special experimental configurations. We circumvented this limitation by synthesizing our reactive solids as thin coatings (only several monolayers thick) on an inert, high surface area substrate. High surface area silica (SiO_2) was coated with pyrolusite at a surface coverage of 0.10 wt% MnO_2 (0.06 wt% Mn). This surface coverage allowed for multiple Mn valence states to be identified without self-absorption effects; details on the

procedure for synthesizing the pyrolusite coated silica ate provided elsewhere (Fendorf et al., 1998).

Briefly, the method for depositing thin films of pyrolusite on silica involved the use of high surface area silica (SiO_2; TIMCO Corp.), with a gram size <44 μm (silt sized and smaller). A 50% w/w reagent grade $Mn(NO_3)_2$ solution was diluted with deionized water to make a solution weighing about 7% of the silica used. After mixing well, this amount of solution just barely dampened the silica, thus dispersing the $Mn(NO_3)_2$. To ensure that the pyrolusite formed a uniform coverage on the silica surface, the mixture was slowly rotated in Teflon vessels at 100°C until the liquid had evaporated. The mixture was baked further at 160°C for 3 days to ensure that pyrolusite had formed. The formation of pyrolusite using this procedure was confirmed using x-ray diffraction and XANES spectroscopy (Fendorf et al., 1998). When the coating process was complete, residual nitrate was washed from the pyrolusite-coated silica using reagent water.

2.2 Flow-Experiments

A horizontal flow cell (rectangular cell with width = 0.4 cm, height = 0.5 cm, and a pathlength = 2.7 cm) was constructed and packed with β-MnO_2 coated silica to a uniform bulk density. The flow cells contained a Mylar window along a portion of the flow field where the x-ray beam could penetrate the sample (Figure 1). The reductant, 0.2 mM $Co(II)EDTA^{2-}$, a Br' tracer , and a background electrolyte of 5.0 mM $CaCl_2$, were added to columns, and the dynamic redox conditions in the flow field were continuously monitored using XANES spectroscopy. The flow rate of the reacting solution was maintained at 1 mL/h, resulting in pore water flux values of 0.3 cm/h. Solution speciation was monitored by collecting effluent in a fraction collector, which was then analyzed using ion chromatography (Taylor and Jardine, 1995). Using this approach we were able to measure solution and solid-phase species continuously during the course of these hydrodynamic reactions. Possible contributions from solution species in the XANES spectra could be subtracted

spectrally. However, previous studies have noted that no soluble Mn products are formed from the reaction of β-MnO_2 with $Co(II)EDTA^{2-}$; therefore, subtracting solution contributions was not necessary.

2.3 XANES Analysis

X-ray absorption near-edge structure (XANES) spectroscopy was performed on beamline 4-2 (an 8-pole wiggler line) at the Stanford Synchrotron Radiation Laboratory (SSRL), running under dedicated conditions. The ring operated at 3 GeV with a current ranging from ≈ 100 mA to ≈ 50 mA. Energy selection was accomplished using a Si(111) monochromator and was run with a focused beam. XANES spectra were recorded by fluorescent x-ray production using a wide-angle ionization chamber (Stem and Heald, 1979); incident and transmitted intensities were also measured with in-line ionization chambers. Scattered primary radiation was restricted from entering the fluorescent detector by placing a Cr filter in front of the detector.

Extruded columns reacted with $Co(II)EDTA^{2-}$ were initially used to determine the species of manganese after pyrolusite was reacted with $Co(EDTA)^{2-}$, in which a linear set of standard manganese minerals (including all known forms of trivalent Mn hydrous oxides) were fit to the unknown spectra (Fendorf et al., 1998). This approach is similar to methods used to quantify sulfur, arsenic and selenium species in complex media using XANES spectroscopy (Waldo et al., 1991; Vairavamurthy et al., 1994; Pickering et al., 1995; Foster et al., 1998). We observed that a reduced layer of α-Mn_2O_3 developed on the β-MnO_2 surface (Fendorf et al., 1998).

In order to minimize the elapsed time of the reaction during each scan for experiments involving real-time XANES analysis under hydrodynamic flow (in ***situ*** speciation), in this study we used a short scan period that encompassed key spectral features needed to quantify the Mn fraction within the solid-phase. We collected spectra over the energy range 6500 to 6650 eV, with small (0.3 eV) energy steps only between 6545 and 6565 eV. This resulted in

a total scan period less than 3 min and allowed scans to be repeated within 4 minutes. Given that the reaction proceeded for more than 4 h, a 3 min scan time essentially captures the Mn states at a single period during the course of reaction.

To ensure our ability to quantify the proportion of each phase (α-Mn_2O_3 and β-MnO_2) within a mixture using short scans needed for the real-time measurements, we ma& a series of standards having known proportions of each. The mixtures had molar β-MnO_2 to Mn_2O_3 ratios of 1.0:0.0, 0.75:0.25, 0.50:0.50, 0.25:0.75, and 0.0:1.0 (Figure 2). Two prominent peaks centered at 6552.1, and 6557.3 eV were noted in the first derivative spectra of the mixtures containing both Mn minerals. The proportion of 'these peaks also changes with corresponding changes in the proportion of the Mn minerals. We used a series of Gaussian-Lorentzian lines to deconvolute the spectra and to determine their peak areas (A); first derivatives were used to enhance line-shapes and thus improve the sensitivity of the deconvolution method. Relative peak areas were used to represent each phase, with the fraction of pyrolusite (β-MnO_2) represented by (A_{6557} / { A_{6552} + A,,,,)) and that for bixbyite (Mn_2O_3) represented by (1- A_{6557} / { A_{6552} + A_{6557}}). A linear relation (r^2> 0.99) was noted between the relative peak areas and the fraction of each Mn mineral present in the mixture (Figure 3). We used this relationship to quantify the fraction of each mineral within the solid-phase of the columns upon reacting β-MnO_2 with Co(II)EDTA^{2-}.

3. RESULTS

As Co(II)EDTA^{2-} is reacted with pyrolusite-coated silica under dynamic flow conditions, there is a shift in the x-ray absorption K-edge of Mn to a lower energy. The higher energy peak centered at 6557 eV in first-derivative spectra decreases in intensity with a concurrent increase in the intensity of the 6552 eV peak (Figure 4). The low energy contributions arise from the production of α-Mn_2O_3 in the Co(EDTA)-MnO_2 systems (see

Experimental Methods). Quantifying peak areas reveals that the fraction of β-MnO_2, Mn(IV), decreased with the accompanied increase in α-Mn_2O_3, Mn(III) (Figure 5). Breakthrough characteristics of $Co(II)EDTA^{2-}$ and $Co(III)EDTA^{-}$ (Figure 5) were consistent with earlier research (Jardine and Taylor, 1995). Oxidation of cobalt was initially rapid and slowed with continual exposure of $Co(II)EDTA^{2-}$ to the Mn-oxide. The loss of oxidative potential is not caused by the accumulation of Mn^{2+} on the surface, but rather coincides with the development of surface-associated Mn(III). In fact, Mn(III) is produced coincidental with the breakthrough of $Co(II)$-$EDTA^{2-}$ (Figure 5).

The quantity of α-Mn_2O_3 remains very low during the early course of the reaction where $Co(III)EDTA^{-}$ production increases ($t < 1$ h). However, after approximately the first hour of flow, the production of $Co(III)EDTA^{-}$ begins to diminish with a concurrent increase in the α-Mn_2O_3 fraction (Figure 5). A secondary steady-state in $Co(III)EDTA^{-}$ level is then attained ($t > 3$ h) from the slower oxidation rate of $Co(II)EDTA^{2-}$ by Mn_2O_3--or from a limited exposure of β-MnO_2. The diminished quantity of $Co(III)EDTA^{-}$ during the hydrodynamic experiment indicates that the rate of oxidation is decreasing. It therefore appears that the surface association of α-Mn_2O_3 phase, which is produced from the oxidation of $Co(II)EDTA^{2-}$, impedes the redox reaction and limits the quantity of $Co(III)EDTA^{-}$ produced. The formation of a Mn(III) layer that passivates the pyrolusite surface is consistent with the finding that Mn(II) does not inhibit the reactivity of manganese dioxides (Jardine and Taylor, 1995).

Although we cannot directly document the spatial distribution of the Mn_2O_3 on the β-MnO_2 with this procedure, it is probable that the Mn_2O_3 layer is 'well distributed on the β-MnO_2 surface. This hypothesis is based on the initial thin films of pyrolusite coated on silica coupled with the fact that a majority of the Mn is converted to a Mn_2O_3 phase (greater than 65 % within 4 h). Further supporting this premise is the fact that we could not detect changes in Mn speciation in systems having ten times the quantity of Mn on silica--the bulk Mn(IV) swamped the XANES signal. Thus, it appears that a thin, only a few monolayers thick,

surface layer of α-Mn_2O_3 passivates the pyrolusite surface toward the oxidation of Co(II)-$EDTA^{2-}$.

4. DISCUSSION

4.1 Reaction Series

With the direct measurement of α-Mn_2O_3 formed from pyrolusite reduction under oxygenated hydrodynamic conditions we can refine and clarify the general reaction sequences first proposed by Jardine and Taylor (1995). One possible reaction sequence proposed to explain the diminished reactivity of pyrolusite was the production of Mn(II), followed by readsorption of the divalent species and subsequent oxidation to Mn(III)--summarized by the following reactions.

<u>Oxic Reaction Series 1: Reduction to and Re-oxidation of Mn(II)</u>

$$MnO_2 + 2Co(II)EDTA^{2-} + H_2O \xrightarrow[\text{fast}]{} Mn^{2+} + 2Co(III)EDTA^{-} + 4OH \qquad [1]$$

$$Mn^{2+}\ (aq) + MnO_2 \xrightarrow[\text{fast}]{} Mn^{2+}\text{-}MnO_2 \qquad [2]$$

$$4Mn^{2+}(ad) + 8OH^{-} + O_2 \xrightarrow[\text{moderate}]{} 2Mn_2O_3 + 4H_2O \qquad [3]$$

We can dismiss this reaction sequence because at no time did we observed appreciable Mn(II) levels on the solids that would result as a consequence of a rapid adsorption (Rxn 2) followed by a slower oxidation step (Rxn 3). This reaction scenario may, however, be viable with other forms of manganese hydrous oxides or under the special condition of high contaminant concentrations since Mn^{2+} has been observed in the effluent of column displacement experiments involving Co(II)$EDTA^{2-}$ transport in undisturbed soils (Jardine et al., 1993).

Oxic Reaction Series 2: Reduction to Mn(III)

The second reaction series proposed by Jardine and Taylor (1995) for oxic conditions therefore appears to be operational, where Mn(III) is the product (rather than a possible intermediate) in the reduction of pyrolusite by $Co(II)EDTA^{2-}$.

$$2MnO_2 + 2Co(II)EDTA^{2-} + H_2O \xrightarrow[\text{fast}]{} \alpha\text{-}Mn_2O_3 + Co(III)EDTA^{-} + 2OH^{-} \quad [4]$$

Manganese(IV) is regenerated under the conditions of a well oxygenated dynamic solution.

$$2\ \alpha\text{-}Mn_2O_3 + O_2 \xrightarrow[\text{moderate}]{} 4MnO_2 \quad [5]$$

Additionally, the possibility that $\alpha\text{-}Mn_2O_3$ also serves as a suitable, albeit slow, oxidant of Co(II)EDTA2- must be considered.

$$\alpha\text{-}Mn_2O_3 + 2Co(II)EDTA^{2-} + 6H^{+} \xrightarrow[\text{slow}]{} 2Mn^{2+} + 2Co(III)EDTA^{-} + 3H_2O \quad [6]$$

It is unlikely, however, that $\alpha\text{-}Mn_2O_3$ appreciable serves as a reductant under the conditions investigated or again we should detect Mn(II) within the system (either in solution or as an adsorbate, neither of which is observed). Thus, Reactions 4 and 5 appear to be the dominant processes operating under these reaction conditions; the longer-term ($t > 4$ h) rate of $Co(II)EDTA^{2-}$ oxidation thus appears to be dependent (or limited by) the rate of Mn_2O_3 reoxidation to MnO_2.

4.2 Solid-phase Reactivity

Manganese oxides are one of the strongest oxidants naturally present in the environment and have important consequences on the fate of many contaminants, e.g., chromium (Johnson and Xyla, 1991; Fendorf and Zasoski, 1992; Chung et al., 1994), arsenic (Oscarson et al., 1981), cobalt (Murray and Dillard, 1979; Jardine and Taylor,

1995), selenium (Wang et al., 1995), and organic compounds (McBride, 1989; Stone and Ulrich, 1989; Klausen et al., 1997). Diminishing reactivity of manganese minerals toward the oxidation of contaminants with increased reaction time has been widely observed. A postulate explaining this observation is the readsorption of Mn(II) (Amacher and Baker, 1982; McBride, 1989; Stone and Ulrich, 1989). Although the addition of Mn(II) to manganese dioxide suspensions limits the reduction of organic compounds, it has not been demonstrated to diminishing the oxidizing potential toward many inorganic ions including chromium(III) and Co(II) (Fendorf et al., 1993; Jardine and Taylor, 1995). An alternative hypothesis for inhibited oxidative potential illustrated by this research is that a passivating Mn(III) layer, such as α-Mn_2O_3, may develop on manganese dioxide mineral surfaces. Manganese(III) has been identified as a product in the adsorption of Co(II) by manganese dioxides (Crowther et al., 1983); it is also frequently observed as an intermediate or end-product in the oxygenation pathway of Mn(II) (Hem, 1978; Hem and Lind, 1983; Murray et al., 1985; Golden et al., 1986; Junta and Hochella, 1994).

Our observations suggest that the α-Mn_2O_3 layer oxidizes $Co(II)EDTA^{2-}$ much more slowly than the Mn(IV) bearing pyrolusite-more slowly than the molecular oxygen driven reoxidation to MnO_2. This fading contrast the oxidative reactivity of many Mn(III) phases toward both inorganic and organic compounds (Stone and Morgan, 1984; Johnson and Xyla, 1991; Xyla et al., 1992; Chung et al., 1994; Kostka et al., 1995). In fact, Xyla et al. (1992) noted that the thermal oxidation of oxalate was more rapid by γ-MnOOH than β-MnO_2; similarly, Chung et al. (1994) noted that both hausmannite and bimessite oxidized Cr(III) more rapidly than pyrolusite. Manganese(III) is also a common constituent of disordered and highly reactive Mn(IV) phases such as bimessite (Nesbitt and Banerjee, 1998). Nevertheless, under the conditions employed in this study and elsewhere (Jardine and Taylor, 1995; Fendorfet al., 1998), it is clear that the formation of α-Mn_2O_3 occurs on pyrolusite and retards the oxidation of the organo-metallic $Co(II)EDTA^{2-}$ complex.

The low reactivity of α-Mn_2O_3 toward the oxidation of $Co(II)EDTA^{2-}$ can be explained appreciably by an extension of a linear free energy relationship imparting a kinetic effect from a thermodynamic parameter (Moore and Pearson, 198 1). The α-Mn_2O_3 Mn(III) phase is very stable as reflected by its reduction potential (I?'), which is 85 mV lower than for pyrolusite ($E^{o\prime}_{\beta MnO_2}$ = 519 mV; Stone 1987) and 60 mV lower than manganite ($E^{o\prime}_{MnOOH}$ = 494 mV; Stone, 1987) at pH 7 with a Mn(II) concentration of 0.1 mM ($E^{o\prime}_{\alpha\text{-}Mn_2O_3}$ = 434 mV; Bricker, 1965; Pourbaix, 1974). Although not expressed explicitly in Reaction 4, the initial step in the redox reaction would involve adsorption of the $Co(II)EDTA^{2-}$ complex on pyrolusite. By extension from adsorption phenomena of this complex on Fe(III) and Al(III) hydrous oxides (Girvin et al., 1993; Zachara et al., 1995a), adsorption likely results from a ligand exchange process. Thus, the rate of electron transfer may be governed by surface dissociation of pyrolusite and bixbyite, which is reflected by the redox potential of the phase. On this basis, one would expect a slower rate of Mn_2O_3 reduction by Co(II)EDTA than for β-MnO_2. The reductive dissolution rate of Mn(III,IV) oxides by substituted phenols are similarly correlated to the redox potentials of the specific complex (Stone, 1987).

4.2 Experimental Attributes

The success of the experiments documented above primarily result from the method used to prepare the MnO_2 solid phase. By preparing a thin coating of the MnO_2 mineral on a high surface area substrate (i.e. silt sized and smaller silica), it is possible to detect Mn reduction products in the presence of the original oxidized mineral. Because the redox reaction is surface mediated, too much of the Mn(IV) mineral will mask the detection of the

Mn(III) or Mn(II) reduction products. This was the case for time-resolved experiments performed in-line using a 10x higher concentration of MnO_2 coated silica (1.0% vs. 0.1% coating) and $Co(II)EDTA^{2-}$ (2.0 mM vs. 0.2 mM). Even though the ratio of the solid phase Mn and the reductant were constant, Mn reduction products were not detected due to the overwhelming signal of the Mn(IV) (data not shown). These sets of experiments add credibility to 'the notion that oxidation of $Co(II)EDTA^{2-}$ by Mn-oxides is a surface-mediated process that is restricted to the outer molecular layers of the mineral structure.

Our approach for discerning the solid-phase transformations used time-resolved spectroscopy to assess dynamic geochemical processes during saturated flow through porous media. These results document for the first time that XANES spectroscopy can be coupled with hydrodynamic reaction flow cells to quantify subtle changes in solid-state geochemistry in the presence of redox reactive contaminants. This work also represents the first *in situ* identification of a Mn(III) layer on MnO_2 under hydrodynamic conditions that explains its redox inactivity.

Experimental Attributes

This research was funded by the Laboratory Directed Research and Development Program of the Oak Ridge National Laboratory and the Subsurface Science Program of the Office of Biological and Environmental Research, U.S. Department of Energy, under contract DE-AC05-96OR22464 with Lockheed Martin Energy Corporation. The authors appreciate the efforts of Dr. Frank Wobber, the contract officer for the Department of Energy, who partially supported this work. We also gratefully acknowledgethe staff and scientists at the Stanford Synchrotron Radiation Laboratory (SSRL) for their help in conducting the XANES analyses. SSRL is operated by the Department of Energy, Office of Basic Energy Sciences. The SSRL Biotechnology Program is supported by the National Institutes of Health, National Center for Research Resources, Biomedical Technology Program, and by the Department of Energy, Office of Biological and Environmental Research.

REFERENCES

Amacher M.C. and Baker D.A. Redox reactions involving chromium, plutonium, and manganese in soils, final report DE-ASO8-77DPO45 15; Institute for Research on Land & Water Resources, Penn. State University. (1982).

Bricker 0: (1965) Some stability relations in the system $Mn-O_2-H_2O$ at 25°C and one atmosphere total pressure. ***Am. Mineral. 50,*** 1296-1354.

Brooks S. C. Taylor D. L. and Jardine P. M. (1996) Reactive transport of EDTA-complexed cobalt in the presence of ferrihydrite. ***Geochim. Cosmochim. Acta 60:*** 1899-1908.

Chung J.-B. Zasoski, R.J. and Lim S.-U. (1994) Kinetics of chromium(III) oxidation by various manganese oxides. ***Korean Agri. Chem. Biotech.*** 37, 414-420.

Crowther D.L., Dillard J.G., and Murray J.W. (1983) The mechanism of Co(II) oxidation on synthetic bimessite. ***Geochim. Cosnwchim. Acta 47,*** 1399-1403.

Fendorf S. Jardine P.M. Taylor D.L. Brooks ***S.C.*** and Rochette E.A. ***in Kinetics and Mechanisms of Reactions at the Mineral-water Interface*** (eds Sparks, D.L. & Grundl, T.). American Chemical Society; Washington, D.C. (1998). In press.

Fendorf S.E. and Zasoski, R.J. (1992) Chromium(III) oxidation by δ-MnO_2. I: Characterization. ***Environ. Sci. Technol.*** **26**, 79-85.

Fendorf S.E. Zasoski R.J. and Burau R.G. (1993) Competing metal ion influences on chromium(III) oxidation by bimessite. ***Soil Sci. Soc. Am. J.*** **57**, 1508-15 15.

Foster A.L. Brown G.E., Jr. and Parks G.A. (1998) X-ray absorption fine-structure spectroscopy study of photocatalyzed, heterogeneous As(III) oxidation on kaolin and anatase. ***Environ. Sci. Technol. 32,*** 1444-1452.

Francis A. J. Iden C. R. Nine B. J. and Chang C. K. (1980) Characteristics of organics in leachate from the low-level radioactive waste disposal sites. *Nucl. Technol.* **50,** 158-163.

Girvin D.C. Gassman P.L. and Bolton H., Jr. (1993) Adsorption of aqueous cobalt ethylenediaminetetraacetate by δ-Al_2O_3. *Soil Sci. Soc. Am, J.* **57,** 1- 11.

Golden D.C. Dixon J.B. and Chen C.C. (1986) Ion exchange,thermal transformation, and oxidizing properties of bimessite. *Clays Clay Minerals* **34,** 5 1 l-520.

Healy T.W. Herring A.P. and Fuerstenau D.W. (1966) The effect of crystal structure on the surface properties of a series of manganese dioxides. *J. Colloid Interface Sci.* **21**, 435-444.

Hem, J. D. (1978) Redox processes at the surfaces of manganese oxide and their effects on aqueous metal ions. *Chem. Geol.* **21,** 199-218.

Hem, J.D. (198 1) Rates of manganese oxidation in aqueous systems. *Geochim. Cosmochim. Acta* **45, 1369-1374.**

Hem, J.D., and Lind C.J. (1983) Nonequilibrium models for predicting forms of precipitated manganese oxides. *Geochim Cosmochim Acta* **47, 2037-2046.**

Hem J.D. Roberson C.E. and Foumier R.B. 1982. Stability of βMnOOH and manganese oxide deposition from springwater. *Water Res. Research* **18**, 563-570.

Jardine P.M. Jacobs G.K. and O'Dell J.D. (1993) Unsaturated transport processes in undisturbed heterogeneous porous media: II. Co-contaminants. *Soil Sci. Soc. Am. J.* **57**, 954-962.

Jardine P.M. and Taylor D. L. (1995) Kinetics and mechanisms of cobalt(II)EDTA oxidation by pyrolusite. *Geochim. Cosmochim. Acta.* **59**, 4193-4203.

Johnson C.A. and Xyla A.G. (1991) The oxidation of chromium(III) to chromium(VI) on the surface of manganate (γ-MnOOH). ***Geochim Cosmochim Acta.*** **55,** 2861-2866.

Junta J.L. and HochellaM.F., Jr. (1994) Manganese (II) oxidation at mineral surfaces: A microscopic and spectroscopic study. ***Geochim. Cosmochim. Acta*** **58,** 4985-4999.

Killey R.W.D. McHugh J.O. Champ D.R. Cooper E.L. and Young J.L. (1984) Subsurface cobalt-60 migration from a low-level waste disposal pit. ***Environ. Sci. Technol.*** **18,** 148-157.

Klausen J. Haderlein S.B. and Schwarzenbach R.P. (1997) Oxidation of substituted analines by aqueous MnO_2: Effect of co-solutes on initial and quasi-steady-state kinetics. ***Environ. Sci. Technol.*** **31,** 2642-2649.

Kostka J.E. Luther G.W., III and Nealson K.H. 1995. Chemical and biologicalreduction of Mn(III)-pyrophosphate complexes: Potential importance of dissolved Mn(III) as an environmental oxidant. ***Geochim. Cosmochim. Acta*** **59,** 885-894.

McBride M.B. (1989) Oxidation of 1,2- and 4-dihydroxybenzene by bimessite in acidic aqueous suspension. ***Clays Clay Minerals*** **37,** 479-486.

Means J.L. Crerar D.A. Borscik M.P. and Duguid J.O (1978) Adsorption of Co and selected actinides by Mn and Fe oxides in soils and sediments. ***Geochim. Cosmochim. Acta. 42, 1763-1773.***

Moore J.W. and Pearson R.G. (198 1) ***Kinetics and Mechanisms.*** Wiley and Sons, NY.

Murray J.W. and Dillard J.G. (1979) The oxidation of cobalt(B) adsorbed on manganese dioxide. ***Geochim. Cosmochim. Acta*** **43,** 78 ***I-787.***

Murray J.W. Dillard J.G. Giovanoli R. Moers H. and Stumm W. (1985) Oxidation of Mn(II): *Initial mineralogy,* oxidation *state* and aging. *Geochem. Cosmochim. Acta 49,* 463-470.

Nesbitt H.W. and Banejee D. (1998) Interpretation of XPS Mn(2p) spectra of Mn oxyhydroxides and constraints on the mechanism of MnO_2 precipitation. *Am. Mineral* 83,305,3 15.

Olsen C. R. Lowry P. D. Lee S. Y. Larsen I. L. and Cutshall N. H. (1986) Geochemical and environmental processes affecting radionuclide migration from a formerly used seepage trench. *Geochim. Cosmochim. Acta.* **50**, 593-607.

Oscarson D.W. Huang P.M. Defosse C. and Herbillon A. (1981) Oxidative power of Mn(IV) and Fe(III) oxides with respect to As(III) in terrestrial and aquatic environments. *Nature* **291**, 50-5 1.

Pickering I. J. Brown G. E., Jr. and Tokunaga T. K.. (1995) Quantitative speciation of selenium in soils using X-ray absorption spectroscopy. *Environ. Sci. Technol. 29, 2456-2459.*

Pourbaix M. *(1974) Atlas of Electrochemical Equilibria in Aqueous Solution.* Nat. Assoc. Corrosion Engineers.

Stem E.A. and Heald S.M. (1979) X-ray filter assembly for fluorescence measurements of x-ray absorption fine structure. *Rev. Sci. Intrum.* 50, 1579-1582.

Stone A.T. (1987) Reductive dissolution of manganese(III)/IV) oxides by substituted phenols. *Environ. Sci. Technol. 21, 979-988.*

Stone A.T. and Ulrich H.-J. (1989) Kinetics and reaction stoichiometry in the reductive dissolution of manganese(IV) dioxide and Co(III) oxide by hydroquinone. *J. Colloid Interface Sci.* **132**, 509-522.

Stone A.T. and Morgan J.J. (1984) Reduction and dissolution of manganese(III) and manganese(IV) oxides by organics. 2. Survey of the reactivity of organics. *Environ. Sci. Technol.* 18, 6 17-624.

Szecsody J.E. Zachara J.M. and Bruckhart P.L. (1994) Adsorption-dissolution reactions affecting the distribution and stability of Co(II)EDTA in iron oxide-coated sand. *Environ. Sci. Technol. 28,* 1706- *17 16.*

Taylor D.L. and Jardine P.M. (1995) Analysis of cobalt(II)EDTA and cobalt(III)EDTA in pore water by ion chromatography. *J. Environ. Qual.* **24**, 789-792.

Vairavamurthy A., Zhou W. Eglinton T. and Manowitz B. (1994) Sulfonates: a novel class of organic sulfur compounds in marine sediments. *Geochim. Cosmochim. Acta 58,* 468 l-4687.

Waldo G.S. Carlson R.M.K. Moldowan J.M. Peters D.E. and Penner-Hahn J.E. (1991) Sulfur speciation in heavy petroleums: Information from X-ray absorption near-edge structure. *Geochim. Cosmochim. Acta* **55**, 80 l-8 14.

Wang B. and Burau R.G. (1995) Oxidation of dimethylselenide by δ-MnO_2: Oxidation product and factors affecting oxidation rate. *Environ. Sci. Technol. 29,* 1504- 15 10.

Xue Y. and Traina S.J. (1996) Oxidation kinetics of Co(II)-EDTA in aqueous and semi-aqueous goethite suspensions. *Environ. Sci. Technol.* 30, 1975- 198 1.

Xyla A.G. Sulzberger B. Luther G.W., III Hering J.G. Van Cappellen P. and Stumm W. 1992. Reductive dissolution of manganese(III,IV) (hydr)oxides by oxalate: The effect of pH and light. *Langmuir* **8**, 95-103.

Zachara J.M. Gassman P.L. Smith S.C. and Taylor D. (1995a) Oxidation and adsorption of $Co(II)EDTA^{2-}$ complexes in subsurface materials with iron and manganese oxide grain coatings. *Geochim. Cosmochim. Acta* **5**, 4449-4463.

Zachara J.M. Smith S.C. and Kuzel L.S. (1995b) Adsorption and dissociation of Co-EDTA complexes in iron oxide-containingsubsurface sands. *Geochim. Cosmochim. Acta* **59**, 4825-4839.

LIST OF FIGURES

Figure 1. Schematic illustration of experimental configuration for ***in-situ*** measurement of solid-phase species under hydrodynamic reaction conditions.

Figure 2. First-derivative Mn-XANES spectra for a series of standards with varying molar ratios of β-MnO_2 to Mn_2O_3.

Figure 3. Relative peak areas (described in text) for varying molar fractions of β-MnO_2 and Mn_2O_3, illustrating the linear relation used to quantify each phase in unknown spectra.

Figure 4. First derivative Mn-XANES spectra during the reduction of β-MnO_2 by $Co(II)EDTA^{2-}$, showing the change in relative peak areas centered at energies of 6552 and 6557 eV. The increased intensity of the low energy peak relative to the diminished intensity of the high energy peak corresponds to the production of Mn_2O_3 denoted in Figure 5.

Figure 5. Aqueous cobalt and solid-phase manganese speciation during the reactive transport of $Co(II)EDTA^{2-}$ through packed mineral beds of β-MnO_2 coated silica (pH=6.5 and q=0.3 cm/h). Relative fractions of Mn(III) (as α-Mn_2O_3) and $Co(III)EDTA^-$ produced during the reactions are measured in real-time.

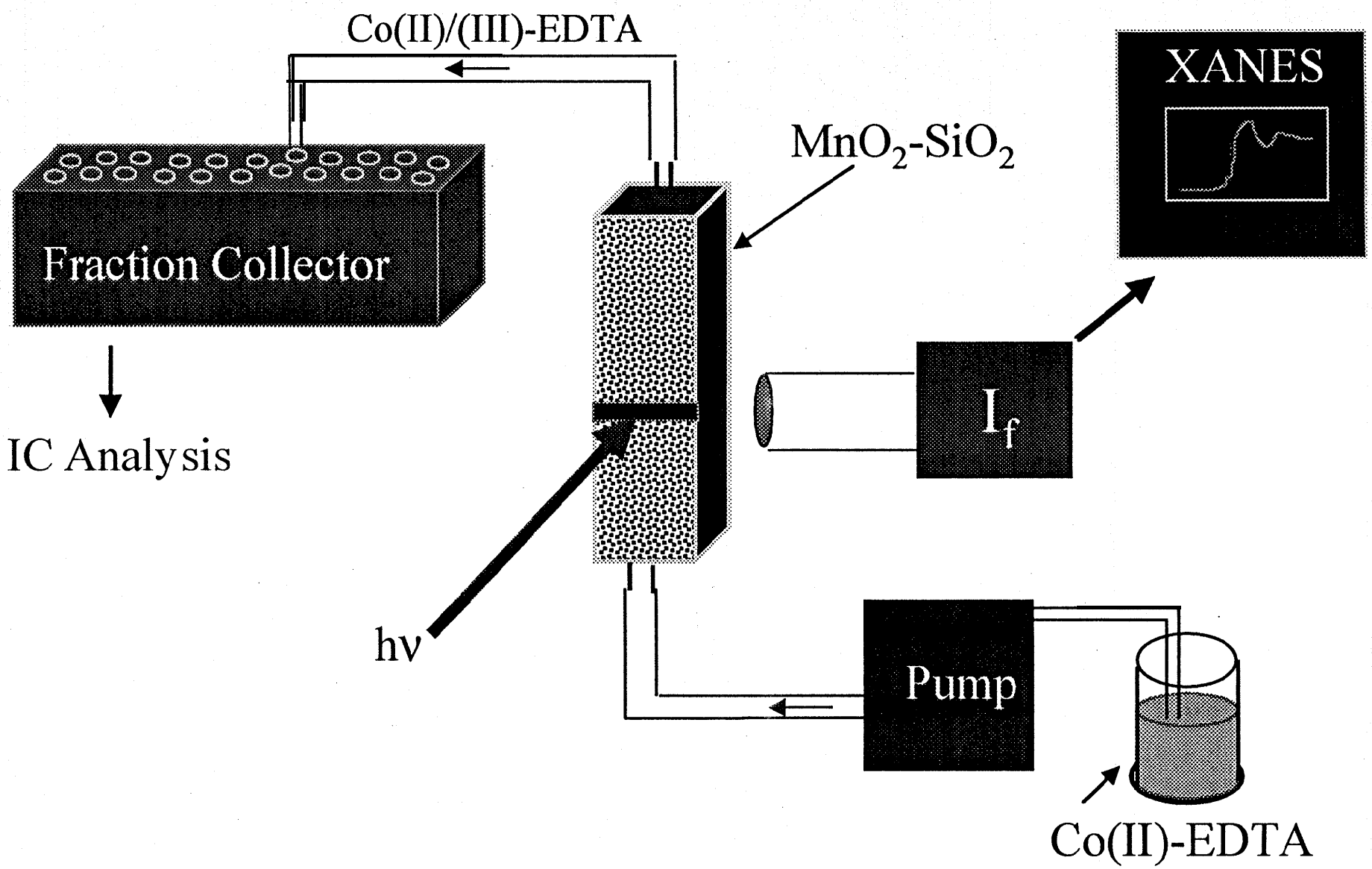
Co(II)/(III)-EDTA
XANES
MnO_2-SiO_2
Fraction Collector
IC Analysis
I_f
hν
Pump
Co(II)-EDTA

Figure 1

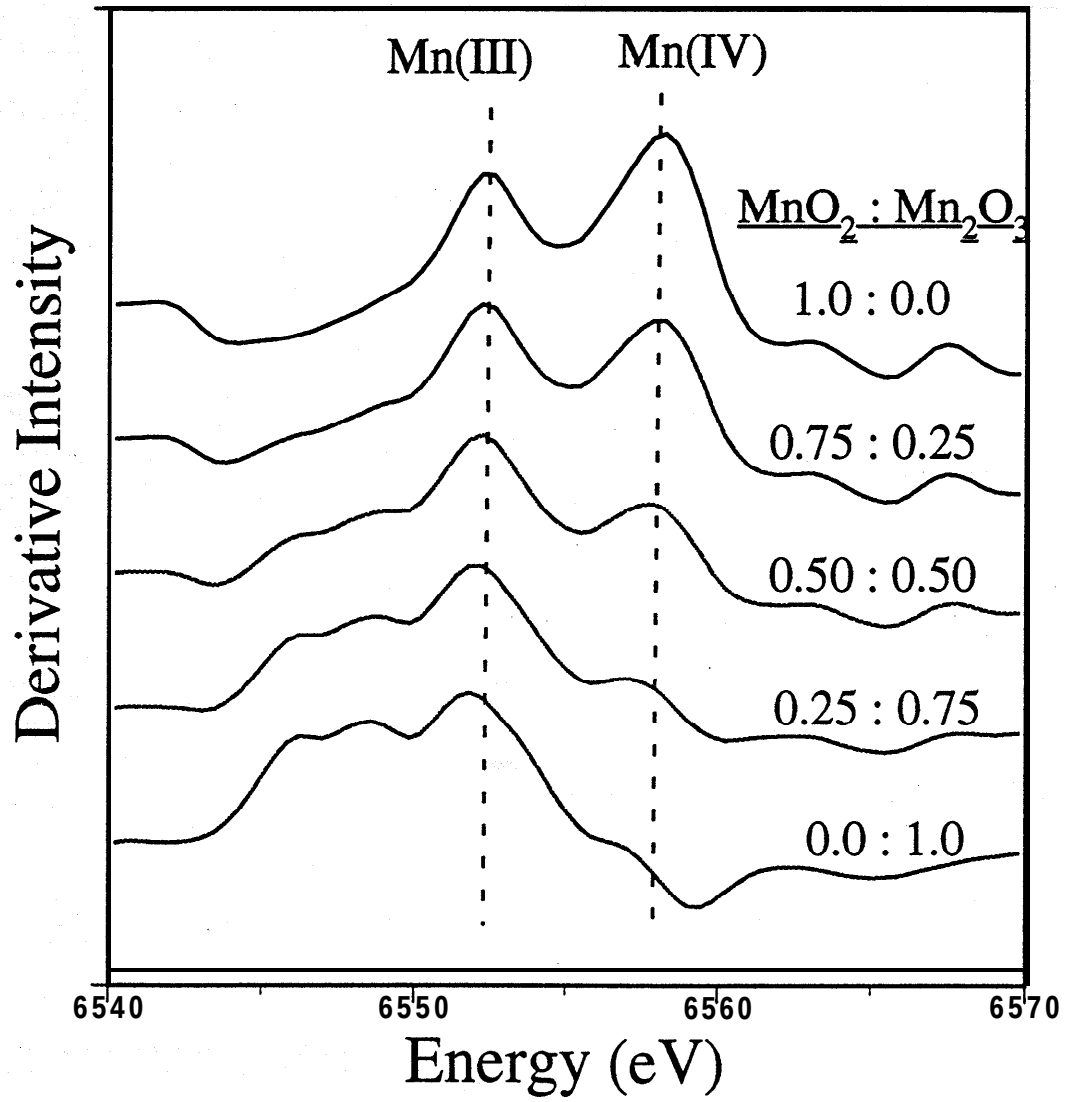
Mn(III)
Mn(IV)
MnO2 : Mn2O3
1.0 : 0.0
0.75 : 0.25
0.50 : 0.50
0.25 : 0.75
0.0 : 1.0
Derivative Intensity
6540
6550
6560
6570
Energy (eV)

Figure 2

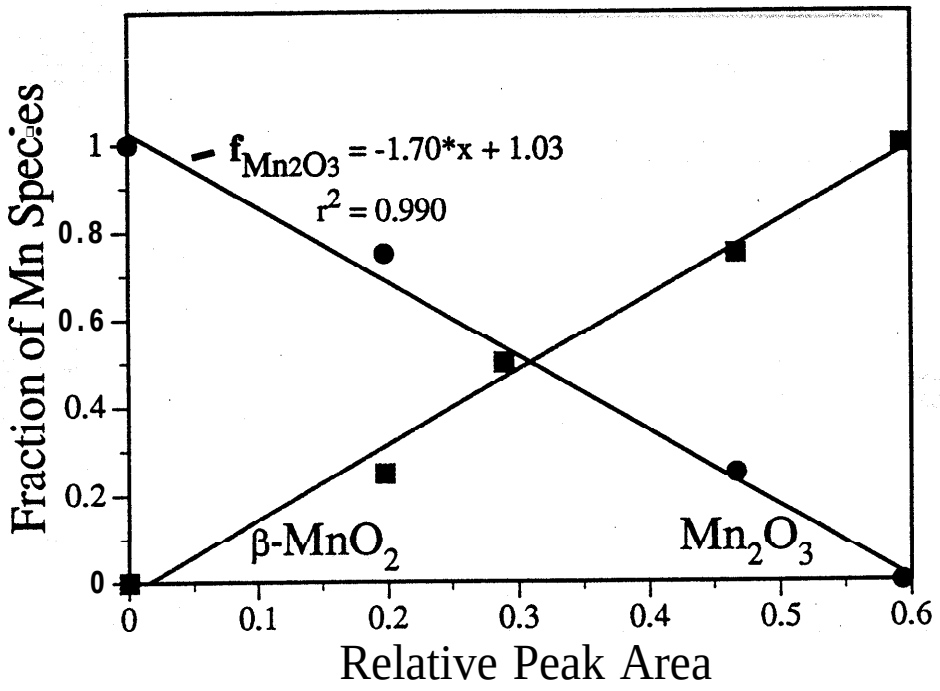
Fraction of Mn Species
1
0.8
0.6
0.4
0.2
0
$f_{Mn2O3} = -1.70*x + 1.03$
$r^2 = 0.990$
β-MnO_2
Mn_2O_3
0
0.1
0.2
0.3
0.4
0.5
0.6
Relative Peak Area

Figure 3

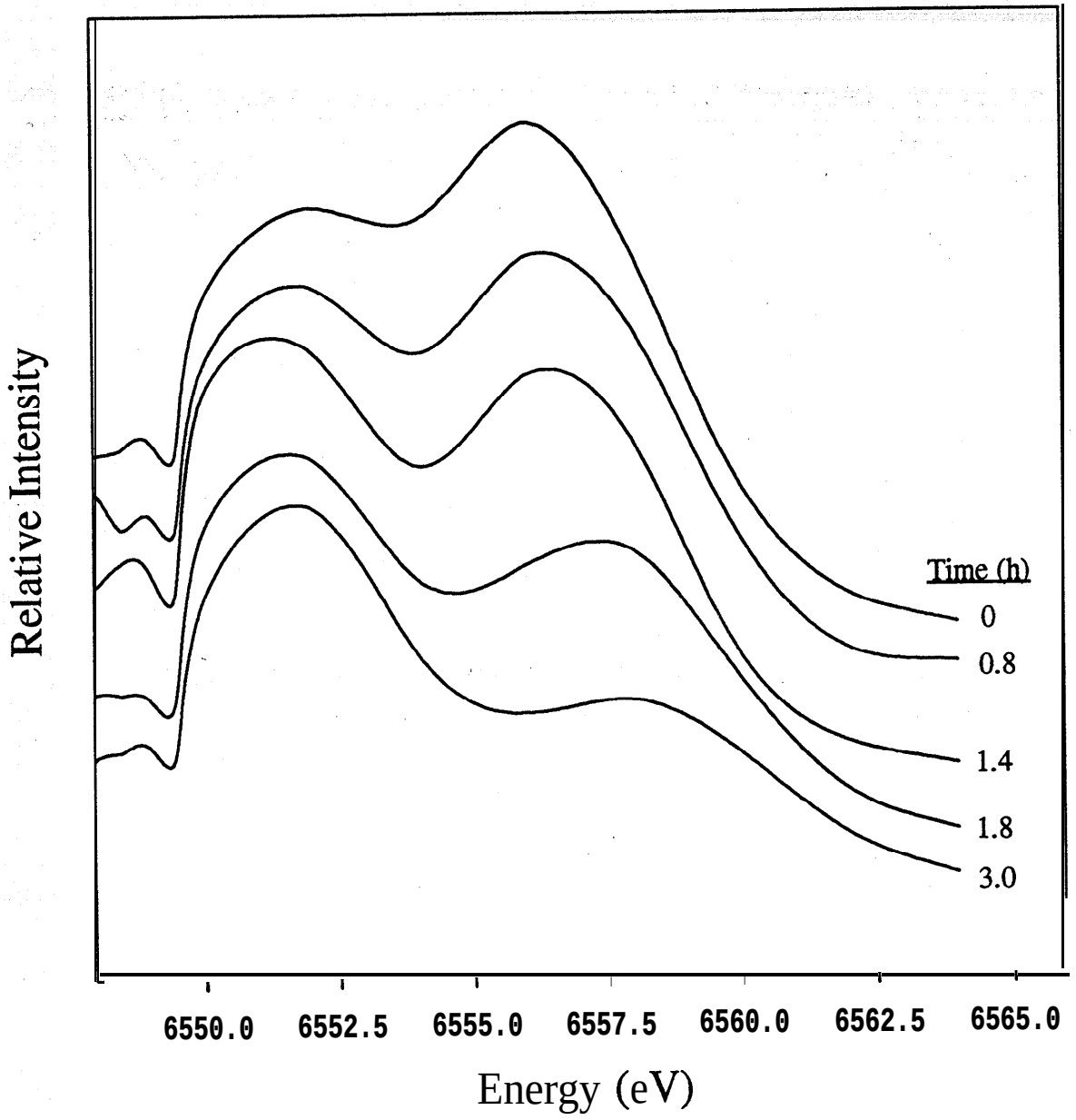
Relative Intensity
Time (h)
0
0.8
1.4
1.8
3.0
6550.0
6552.5
6555.0
6557.5
6560.0
6562.5
6565.0
Energy (eV)

Figure 4

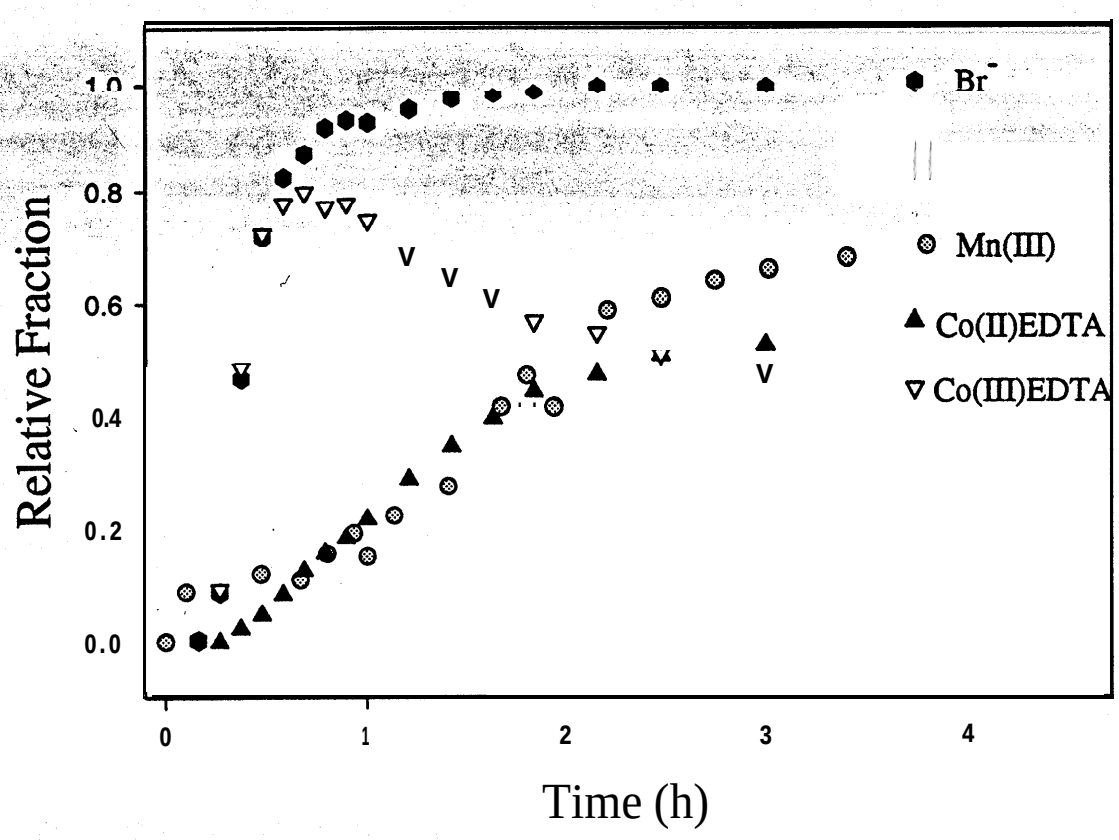
Relative Fraction
1.0
0.8
0.6
0.4
0.2
0.0
0
1
2
3
4
Time (h)
Br⁻
Mn(III)
Co(II)EDTA
Co(III)EDTA

Figure 5